



## Copper-based nanoparticles prepared from copper(II) acetate bipyridine complex

TATIANA A. LASTOVINA<sup>1\*</sup>, ANDRIY P. BUDNYK<sup>1</sup>, GEVORG A. KHAISHBASHEV<sup>1</sup>, EGOR A. KUDRYAVTSEV<sup>2</sup> and ALEXANDER V. SOLDATOV<sup>1</sup>

<sup>1</sup>*International Research Center “Smart materials”, Southern Federal University, 344090, 5, Zorge Str., Rostov-on-Don, Russia and <sup>2</sup>Joint Research Center “Diagnostics of structure and properties of nanomaterials”, Belgorod National Research University, 308015, 85, Pobedy Str., Belgorod, Russia*

(Received 11 December 2015, revised 17 March, accepted 29 March 2016)

**Abstract:** The syntheses of CuO, Cu/Cu<sub>2</sub>O and Cu<sub>2</sub>O/CuO nanoparticles (NPs) from a single copper(II) acetate bipyridine complex by three different methods, microwave-assisted, solvothermal and borohydride, are reported. The presence of the bipyridine ligand in the copper complex would impose no necessity for additional stabilization during synthesis. The phases of formed NPs were identified by X-ray diffraction. The CuO NPs obtained *via* solvothermal synthesis from alkaline solution at 160 °C were of ≈11 nm in size. Cu/Cu<sub>2</sub>O NPs of ≈80 nm were produced *via* a microwave-assisted polyol procedure at 185–200 °C, where ethylene glycol could play a triple role as a solvent, a reducing agent and a surfactant. Cu<sub>2</sub>O/CuO NPs of ≈16 nm were synthesized by a borohydride method at room temperature. The interplanar spacing calculated from selected-area electron diffraction data confirmed the formation of Cu, CuO and Cu<sub>2</sub>O phases in the respective samples. All NPs were stable and could be used for various applications, including biomedicine.

**Keywords:** Copper(II) acetate complex; copper and copper oxides nanoparticles; solvothermal and microwave-assisted polyol synthesis; borohydride method.

### INTRODUCTION

Recently, copper, cupric oxide (CuO) and cuprous oxide (Cu<sub>2</sub>O) NPs have gained much attention due to their particular physical and chemical properties.<sup>1</sup> They are widely used in areas of catalysis<sup>2</sup> and environmental remediation,<sup>3</sup> in optical and magnetic devices,<sup>4</sup> in nanofluids of heat exchangers<sup>5</sup> and as antibacterial agents.<sup>6</sup> Copper-based NPs can be prepared by several methods, such as chemical reduction,<sup>7</sup> thermal decomposition,<sup>8</sup> microwave-assisted,<sup>9</sup> solvother-

\* Corresponding author. E-mail: lastovina@sfedu.ru  
doi: 10.2298/JSC151211036L

mal<sup>10</sup> and electrochemical synthesis,<sup>11</sup> biosynthesis,<sup>12</sup> and by some physical methods.<sup>13</sup> The most conventional method is the reduction of a copper complex in the presence of a capping agent. The reducing agents are hydrazine hydrate, tetrahydroborates, hypophosphites, formaldehyde, methanol, citrates,<sup>14</sup> while ethylenediamine, allylamine, cetyltrimethylammonium bromide, tetraoctylammonium bromide, poly(vinyl pyrrolidone), tetraethylengenetamine, sodium dodecylbenzenesulphonate are used as capping agents.<sup>15,16</sup> It is worth mentioning that the preparation of CuO or Cu NPs from copper acetate without additional stabilization leads to the formation of aggregates or large-size NPs.<sup>17,18</sup> Organic compounds, such as L-ascorbic acid, possessing both reducing and capping properties are promising reagents for the synthesis of well-dispersed Cu/CuO NPs.<sup>19</sup>

The most difficult task is to prepare pure copper NPs because copper easily oxidizes in air to form copper oxides. In order to prevent this, copper NPs are usually prepared encapsulated in organic or inorganic materials, such as carbon, silica and multi-layered graphene,<sup>20</sup> or a polymer matrix.<sup>21</sup> Alternatively, the synthesis could be performed in an anaerobic solution under an atmosphere of argon or nitrogen, or in non-aqueous solvents. Arul Dhas *et al.*<sup>22</sup> prepared nano-scale copper clusters by the thermal and ultrasound-assisted reduction of copper hydrazinecarboxylate in water. Thermal reduction at 80 °C under an argon atmosphere resulted in irregular agglomerated copper NPs of 200–300 nm, while a sonochemically derived product showed the presence of both Cu and Cu<sub>2</sub>O NPs of ~50 nm in size. Fan *et al.*<sup>23</sup> used the precipitation–pyrolysis method focusing on the synthesis of monodispersed CuO nanocrystals (7–30 nm) starting from basic copper carbonate precursors, prepared from copper acetate or copper sulfate. Unfortunately, such studies were limited to a single adopted synthetic route and hence, did not reveal the full potential of the chosen metal complex.

Copper(II) salts such as chlorides, sulfates, acetates, nitrates and carbonates are normally used to obtain families of copper and copper oxides NPs (see Supplementary material to this paper, Table S-I). Only a few examples were found where different copper oxides were produced from a copper complex, containing different ligands. The first to mention is the copper dimethylglyoximate complex, employed by Zhang *et al.*<sup>24</sup> to produce hydrothermally Cu<sub>2</sub>O microcrystals, which motivated Purkayastha *et al.*<sup>8</sup> to use the bis(dimethylglyoximato)copper(II) complex for the synthesis of 28.9 nm (by XRD) CuO NPs by thermal decomposition at 220 °C. Cationic copper(II) Schiff base complexes is another family to note, referring to recent report of Ebrahimipour *et al.*<sup>25</sup> where CuO NPs of 23 nm size (by XRD) were obtained by calcination at 600 °C for 2 h in air of a novel [Cu(L)(H<sub>2</sub>O)]NO<sub>3</sub>] complex (ligand HL = (E)-N'-(2-hydroxynaphthalen-1-yl)methylene)acetohydrazide). There are no systematic studies so far where the same copper complex was used to produce a variety of copper-based NPs using several synthetic methods.

Polypyridines comprise a class of ligands that have been employed widely in the synthesis of metal complexes for therapeutic uses in cancer treatment.<sup>26</sup> A chelating copper complex containing both bipyridine and acetate ligands could be a promising candidate for the synthesis of copper NPs. In this regard, the  $[\text{Cu}(\text{CH}_3\text{COO})_2(\text{bpy})]$  complex obtained by Koo<sup>27</sup> seemed to be particularly relevant.

In this study, copper-based NPs were prepared from the  $[\text{Cu}(\text{CH}_3\text{COO})_2(\text{bpy})]$  complex by two high temperature methods, *i.e.*, solvothermal and microwave-assisted (MW-assisted), and by the room temperature borohydride method. The presence of the bipyridine ligand in the copper complex imposed no necessity for additional stabilization, while the fast MW-heating or the strong reducing agent allowed acceleration of the synthesis running without an inert atmosphere.

## EXPERIMENTAL

### Materials and measurements

Reagents copper(II) acetate monohydrate ( $\text{Cu}(\text{OAc})_2 \cdot \text{H}_2\text{O}$ ), 2,2'-bipyridine (bpy), dimethylformamide (DMF), sodium borohydride, sodium hydroxide, ethanol and ethylene glycol were purchased from commercial suppliers and used without further purification. Deionized (DI) water (18 MΩ cm) was obtained from a Simplicity UV system.

X-Ray diffraction (XRD) patterns were collected with an Ultima IV powder diffractometer (Rigaku) using  $\text{CuK}_\alpha$  radiation ( $\alpha = 1.5406 \text{ \AA}$ ) with a  $0.02^\circ 2\theta$  step size and a 2 s dwell time. Transmission electron microscopy (TEM) images were acquired on a JEM-2100 microscope (JEOL) operated at an accelerating voltage of 200 kV. The samples were prepared by dropping a dilute NP dispersion in 2-propanol on an amorphous carbon-coated copper grid and allowing it to dry at room temperature. Selected-area electron diffraction (SAED) patterns were also recorded. The optical properties were measured in the diffuse reflectance (DRUV–Vis) mode on a UV-2600 UV–Vis spectrophotometer (Shimadzu). Samples were mixed with  $\text{BaSO}_4$  powder and pressed in the sample holder for an integrating sphere attachment. The Fourier transform infrared (FTIR) spectra were recorded in the transmittance mode using an FSM-1202 FTIR Spectrometer (InfraSpec) under air in KBr pellets.

### Synthesis

*Synthesis of the copper(II) acetate bipyridine complex  $[\text{Cu}(\text{OAc})_2(\text{bpy})]$ .* The complex was prepared by a slightly modified method of Koo.<sup>27</sup> In brief, 0.81 g  $\text{Cu}(\text{OAc})_2 \cdot \text{H}_2\text{O}$  was added to 20 mL DMF and mixture was allowed to stir on a magnetic stirrer until dissolution. After addition of 0.43 g bpy in 10 mL DMF, the mixture was left stirring for 8 h. The solid product was separated by sedimentation and washed with diethyl ether. The obtained pale blue powder was dried in a vacuum oven. This material was used as the precursor for the copper-based NPs.

*Synthesis of copper-based nanoparticles.* The solvothermal synthesis started by dissolving 0.012 g NaOH in 10 mL of ethanol. Then, a solution of 0.1014 g  $[\text{Cu}(\text{OAc})_2(\text{bpy})]$  in 50 mL ethanol was added under stirring of the sodium hydroxide solution. The resulting solution was transferred to a teflon-lined stainless steel autoclave (Berghof BR-200 pressure reactor) and heated at 160 °C for 24 h. After cooling to room temperature, the prepared particles were separated by centrifugation, washed with DI water and dried in a vacuum oven at 60 °C overnight. The product has a brownish-black color, characteristic for a copper(II) oxide.

In the MW-assisted polyol synthesis procedure, 15.2 mL of ethylene glycol solution containing 0.030 g [Cu(OAc)<sub>2</sub>(bpy)] was mixed with 3 mL of ethylene glycol solution containing 0.040 g NaOH. The mixture was heated in a MW reactor (Discover SP, CEM) in a sealed glass tube for 30 min at 185°C (or 200 °C). Then, the formed particles were separated by centrifugation, washed with DI water and dried in a vacuum oven at 60 °C overnight. The product appeared red–brownish, a color known for lower oxides of copper. The results for the sample obtained at 185 °C are reported in the main text, while the data concerning the sample produced at 200 °C are presented in the Supplementary material.

It should be emphasized here that in polyol synthesis, ethylene glycol played a triple role, *i.e.*, as the solvent, the reducing agent and the surfactant.<sup>28</sup> The reduction ability of ethylene glycol is temperature-dependent and it was found that in the MW-assisted polyol synthesis, the reaction did not proceed at temperatures lower than 160 °C.<sup>29</sup>

In the borohydride method, a [Cu(OAc)<sub>2</sub>(bpy)] solution was prepared by dissolving 0.1015 g of the complex in 50 mL of ethanol. A sodium hydroxide solution was prepared by dissolving 0.0121 g NaOH in 10 mL of ethanol. Both solutions were stirred separately until full dissolution of the reagents and then combined under stirring. Then, a sodium borohydride solution (0.0460 g in 10 mL of DI water) was added. Prepared black colored suspension was kept under magnetic stirring for 40 min. Finally, the sample was washed with DI water and dried at 60 °C in a vacuum oven.

Borohydrides are very strong reducing agents in alkaline, neutral and acidic media.<sup>14</sup> In aqueous alkaline media, the reduction reaction of copper ions could occur very fast in the following way:<sup>30</sup>



However, without a protective inert gas atmosphere, copper could be oxidized during the synthesis.

## RESULTS AND DISCUSSION

The synthesized [Cu(OAc)<sub>2</sub>(bpy)] complex was characterized by both FTIR and UV–Vis spectroscopies (Fig. 1). The FTIR spectrum contained combined signatures of the OAc and bpy ligands to the Cu center (see the structure of the molecule in Fig. 1). The positions of characteristic bands given in the work of Koo<sup>27</sup> (marked with asterisks in Fig. 1) for the [Cu(CH<sub>3</sub>COO)<sub>2</sub>(bpy)] complex coincided well with the present results (see the Supplementary material for details). The acetate carboxylate group gave the dominating stretching modes  $\nu_{\text{asym}}(\text{COO}^-)$  and  $\nu_{\text{sym}}(\text{COO}^-)$  at 1628 and 1427 cm<sup>-1</sup>, respectively, while the corresponding bending modes were situated at 680 and 629 cm<sup>-1</sup>. The large separation  $\Delta\nu = \nu_{\text{asym}} - \nu_{\text{sym}} = 201$  cm<sup>-1</sup> is indicative for a unidentate geometry of the OAc ligands bonded to copper.<sup>31</sup> Bpy participates with strong bands at 1566, 1477 and 1323 cm<sup>-1</sup> due to C–C and C=C stretching modes in the ring and aromatic C–H bending modes at 770 and 731 cm<sup>-1</sup> (respective stretching modes are visible at wavenumbers over 3000 cm<sup>-1</sup>). The spectrum also contains some vibrational manifestations of Cu–N and Cu–O bonds at 501 and 467 cm<sup>-1</sup>, respectively. The DRUV–Vis spectrum (inset in Fig. 1) is composed of a broad band peaking at 747 nm, which could be ascribed to d–d transitions occurring in

copper, and a high energy envelope below 400 nm containing OAc-to-Cu LCMT transitions and  $\pi$ -transitions of bpy (see the Supplementary material for details). The profile of the optical spectrum matched well with the band positions reported by Koo.<sup>27</sup> Based on the similarity of the characteristic spectral features, it could be assumed that a good structural equivalence between the  $[\text{Cu}(\text{OAc})_2(\text{bpy})]$  complex synthesized herein and that obtained by Koo was reached. A more detailed study of this complex will be published elsewhere.<sup>32</sup>

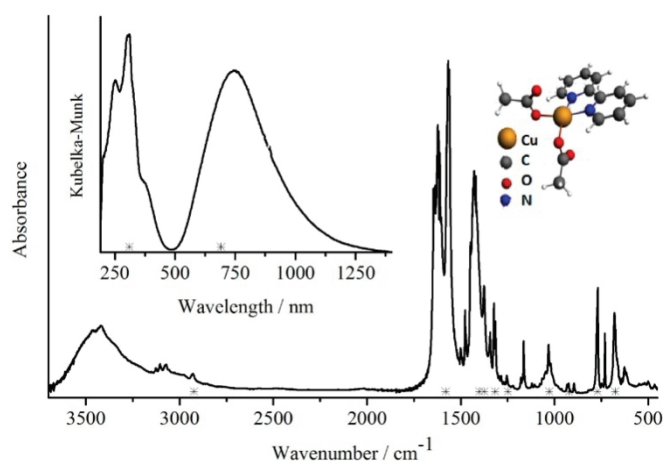


Fig. 1. FTIR and UV–Vis spectra of synthesized  $[\text{Cu}(\text{OAc})_2(\text{bpy})]$ . Asterisks (\*) in the inset indicate the peak positions reported by Koo.<sup>27</sup>

The XRD patterns of the copper-based NPs synthesized from the  $[\text{Cu}(\text{OAc})_2(\text{bpy})]$  complex by the solvothermal, MW-assisted and borohydride methods are presented in Fig. 2. According to the pattern in Fig. 2a, the solvothermal synthesis resulted in the formation of copper(II) oxide phase with average crystallite size of 11 nm, estimated by the Scherrer equation. The MW-assisted polyol synthesis produced copper and copper(I) oxide simultaneously, evidenced by the corresponding XRD pattern (Fig. 2b) containing reflexes attributed to the both phases. The average crystallite size of Cu and  $\text{Cu}_2\text{O}$  particles prepared by MW-assisted polyol synthesis could be estimated as 50.6 and 16.6 nm, respectively. The reaction at the higher temperature ( $200^\circ\text{C}$ ) also resulted in Cu and  $\text{Cu}_2\text{O}$  particles with average widths of 40.7 and 27.1 nm, respectively; the corresponding XRD profile is shown in Fig. S-3 of the Supplementary material. The characteristic peaks for both  $\text{Cu}_2\text{O}$  and CuO phases could be observed in the case of the material prepared by the borohydride method (Fig. 2c). The average crystallite sizes of the  $\text{Cu}_2\text{O}$  and CuO NPs were 13.5 and 14.6 nm, respectively. For all three methods, the calculated values of the main structural parameters of the

obtained NPs are summarized in Table I. The values were found to be in good agreement with literature data for CuO, Cu/Cu<sub>2</sub>O and Cu<sub>2</sub>O/CuO phases.

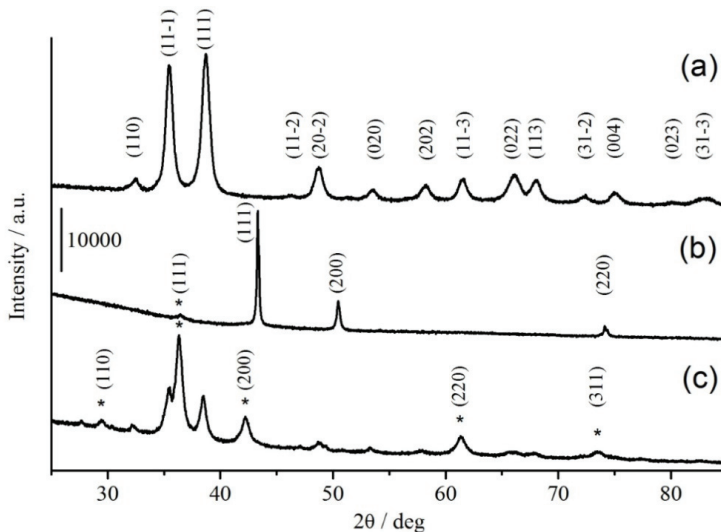


Fig. 2. XRD patterns of the copper-based samples prepared from the [Cu(OAc)<sub>2</sub>(bpy)] complex by solvothermal (a), MW-assisted polyol (b) and borohydride (c) methods. The Miller indices are assigned for reflections of CuO (a, c), Cu (b) and Cu<sub>2</sub>O (b, c) phases, the last is marked with asterisks (\*).

TABLE I. Lattice parameter, *a*, and interplanar spacing, *d*, values for the prepared copper-based NPs. The values were evaluated from XRD and SAED data, and reported with respective reference data (phase and *d*<sub>ICSD</sub>); the value *d*<sub>ICSD</sub> was taken from the Inorganic Crystal Structure Database (ICSD)

Sample	<i>a</i> / Å (XRD)	<i>d</i> / Å <i>d</i> <sub>SAED</sub> / <i>d</i> <sub>ICSD</sub>	Phase ( <i>hkl</i> )	<i>d</i> / Å <i>d</i> <sub>SAED</sub> / <i>d</i> <sub>ICSD</sub>	Phase ( <i>hkl</i> )	<i>d</i> / Å <i>d</i> <sub>SAED</sub> / <i>d</i> <sub>ICSD</sub>	Phase ( <i>hkl</i> )
CuO NPs (solvothermal method)	<i>CuO</i> <i>a</i> =4.695 <i>b</i> =3.4305 <i>c</i> =5.1403	2.5612/ 2.5324	CuO <002>	2.3241/ 2.3243	CuO <111>	1.8731/ 1.8676	CuO <20-2>
Cu/Cu <sub>2</sub> O NPs (MW-assisted method)	<i>Cu</i> <i>a</i> =3.6153 <i>Cu<sub>2</sub>O</i> <i>b</i> =4.2736	2.0917/ 2.0880	Cu <111>	2.1450/ 2.1260	Cu <sub>2</sub> O <002>	1.7928/ 1.8080	Cu <200>
CuO/Cu <sub>2</sub> O NPs (borohydride method)	<i>Cu<sub>2</sub>O</i> <i>a</i> =4.7058 <i>b</i> =3.4407 <i>c</i> =5.1527	3.0609/ 3.0123 <i>CuO</i> <11-3>	Cu <sub>2</sub> O <011>	2.4607/ 2.4595 1.2938/ 1.2959	Cu <sub>2</sub> O <111> <221>	2.1270/ 2.1300 —	Cu <sub>2</sub> O <002> —

The XRD patterns suggest that each method results in a unique product in spite of starting from a common copper precursor. The observations could be preliminary summarized as: 1) products of pure ( $\text{CuO}$ ) and mixed ( $\text{Cu}/\text{Cu}_2\text{O}$  and  $\text{Cu}_2\text{O}/\text{CuO}$ ) phases were obtained, 2) the materials offer a complete line of oxidation states of copper –  $\text{Cu}(0)$ ,  $\text{Cu}(\text{I})$  and  $\text{Cu}(\text{II})$  and 3) the samples contain crystallites in 11–51 nm size range.

TEM analysis was performed in order to gain more detailed information about the morphology of the NPs. Representative TEM micrographs for each sample are presented in Fig. 3 together with particle size distribution histogram and SAED image. As could be seen from Fig. 3a, the solvothermal method produced cubic particles without appreciable structural defects. They covered the 9–15 nm size range with the majority at  $\approx 11$  nm. In the case of the MW-assisted polyol synthesis, round-like (polymorphs of truncated octahedron) particles in the 58–114 nm size range were formed with the majority at  $\approx 82$  nm (Fig. 3b). On careful analysis of images, different types of defects, such as dislocations, twins and stacking faults, were found. Borohydride synthesis resulted in cubic-like NPs with average crystallite size of 16 nm (Fig. 3c) with the whole range of sizes being from 9 to 29 nm. The average size values obtained from processing the TEM images coincided well with the average crystallite sizes evaluated from the XRD data. Calculations of the interplanar spacing,  $d$ , based on SAED and XRD (see Table I and Figs. S-4–S-7 of the Supplementary material) confirmed the formation of the phases previously revealed by powder XRD analysis.

Considering the morphology and size distribution of the NPs, it could be concluded that only solvothermal synthesis resulted in single phase NPs with a narrow size distribution. Borohydride method at the lower temperature and shorter time produces mixed oxides NPs of roughly cubic shape and a broader size distribution (although, remaining close to the average value). The only method capable of leading to the production of a  $\text{Cu}(0)$ -containing product under air was the MW-assisted one, but the particles were 5–10 times larger.

The “as measured” optical spectra of three samples are presented in Fig. 4a in percent of the reflectance values. The observed difference in intensity mostly originated from the non-equivalent amount of sample powder under the light beam. Samples containing  $\text{CuO}$  NPs exhibited a similar broadband profile with maxima at  $\approx 350$  nm for the powder obtained by the solvothermal method and at  $\approx 450$  nm for that using the borohydride method. On the contrary, the optical profile of the MW-assisted sample showed a broad band peaking at  $\approx 550$  nm, the origin of which could be attributed to localized surface plasmon resonance (LSPR) occurring for the copper NPs. This fact itself also gives evidence of the presence of naked copper NPs in the sample after the MW-assisted synthesis.

For a more detailed analysis, these spectra are presented in Fig. 4b as optical density *versus* photon energy (see the Supplementary material for details). The

spectrum of the CuO NPs showed an absorption edge near 1.5 eV, which matches the well known value for this material of 1.45 eV.<sup>33</sup> The spectral curve of the Cu/Cu<sub>2</sub>O NPs had a more complex character; its edge falling near to 2.1 eV and smoothed by a low-energy tail, possibly, due to the presence of structural defects in the particles. The edge position was also close to the characteristic values for Cu<sub>2</sub>O NPs.<sup>34</sup> The last curve shows absorption features typical for both Cu<sub>2</sub>O and CuO materials.

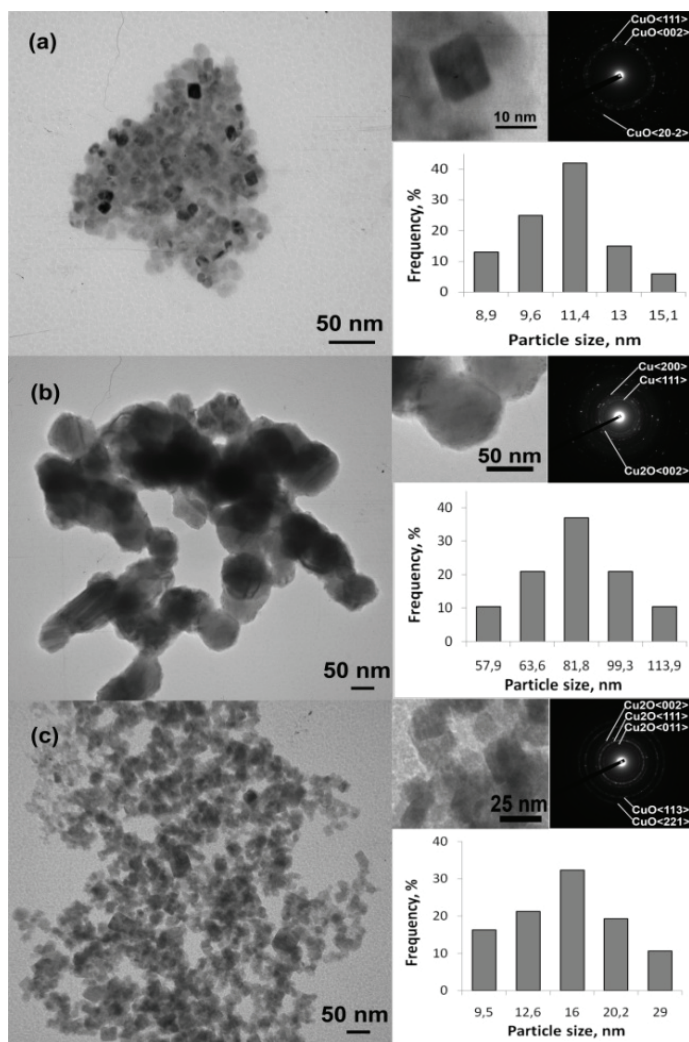


Fig. 3. TEM micrograph, micrograph with a magnified detail, SAED image and particle size distribution histogram for each sample prepared by solvothermal (a), MW-assisted polyol (b) and borohydride (c) methods from  $[\text{Cu}(\text{OAc})_2(\text{bpy})]$  complex. CuO (a), Cu and Cu<sub>2</sub>O (b), and Cu<sub>2</sub>O and CuO (c) phases are indexed in SAED diffraction patterns.

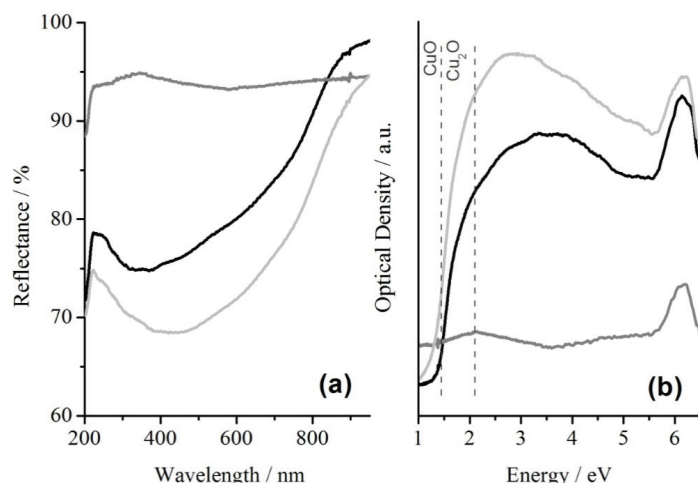


Fig. 4. DRUV–Vis spectra of CuO (black), Cu/Cu<sub>2</sub>O (grey) and Cu<sub>2</sub>O/CuO (light grey) NPs presented in reflectance values *versus* wavelength (a) and as optical density *versus* energy of photons (b).

The solvothermal synthesis, although being slow and energy consuming, is known to offer good control over the particle size distribution and quality in terms of defects. Tang *et al.*<sup>10</sup> obtained Cu<sub>2</sub>O nanocubes of 50–160 nm using ethanol as the reducing agent in alkaline media with PVP in the temperature range 100–150 °C, although claiming the production of Cu–Cu<sub>2</sub>O core–shell NPs at 180 °C. In the present study, pure CuO phase and well-defined NPs were obtained using a mild reducing agent in alkaline media without a capping agent, which is a novel result in the field. It is worth mentioning that the preparation of CuO or Cu NPs from copper acetate without additional stabilization led to the formation of aggregates or large-sized NPs.<sup>17,18</sup> CuO NPs are known for their antimicrobial activity against a range of bacterial pathogens<sup>35</sup> with hospitals and transport as two areas for immediate application to prevent the spread of infections.

Copper is known of being highly sensitive to oxidation by air. In the work of Pastoriza-Santos *et al.*,<sup>36</sup> Cu NPs of ≈48 nm covered by 2 nm layer of Cu<sub>2</sub>O were obtained, and that was interpreted as post-synthesis oxidation during the washing step. It was thought that this layer might prevent, to some extent, further oxidation of the metal core.

Srivastava *et al.*<sup>4</sup> obtained solely Cu<sub>2</sub>O NPs of ≈8 nm by reducing CuSO<sub>4</sub>·5H<sub>2</sub>O with aqueous NaBH<sub>4</sub> at RT in the presence of capping agents. In the present particular case, the borohydride method resulted in a mixture of Cu(I) and Cu(II) oxides, the exact composition of which was difficult to differentiate even though it appeared like a mixture of two types of NPs on the TEM image (Fig. 3c).

## CONCLUSIONS

Copper is considered as a cheap alternative to precious metals, and NPs with controlled size, shape and crystal structure exhibiting long-term stability under air may replace the nobles in a variety of applications. In this regard, the liquid phase protocols adopted here are relatively cheap and simple to scale up. Although a complete understanding of NPs formation remains a challenge, evidence was presented of how a single  $[\text{Cu}(\text{OAc})_2(\text{bpy})]$  complex allowed the preparation of different sets of NPs containing Cu(0), Cu(I), Cu(II). The solvo-thermal method resulted in pure CuO phase of nanocrystallites smaller than both the MW-assisted and the borohydride methods, which produced compositions of Cu/Cu<sub>2</sub>O and Cu<sub>2</sub>O/CuO, respectively. The dry products were stable and could be redispersed in various solvents for further studies.

## SUPPLEMENTARY MATERIAL

Summary of literature review on Cu(II) precursors, IR and UV–Vis spectra of Cu(II) acetate bipyridine complex, XRD patterns and TEM/SAED images for all the samples, a table with the *a* and *d* parameters and DRUV spectra for all the samples are available electronically from <http://www.shd.org.rs/JSCS/>, or from the corresponding author on request.

*Acknowledgements.* This study was financially supported by a grant of Russian Science Foundation (Project № 14-35-00051). The TEM and XRD investigations were performed on scientific equipment at the Joint Research Center “Diagnostics of structure and properties of nanomaterials” of Belgorod National Research University.

ИЗВОД  
НАНОЧЕСТИЦЕ НА БАЗИ БАКРА ДОБИЈЕНЕ ИЗ ДИАЦЕТАТО-БИПИРИДИНБАКАР(II)  
КОМПЛЕКСА

TATIANA A. LASTOVINA<sup>1</sup>, ANDRIY P. BUDNYK<sup>1</sup>, GEVORG A. KHAISHBASHEV<sup>1</sup>, EGOR A. KUDRYAVTSEV<sup>2</sup>  
и ALEXANDER V. SOLDATOV<sup>1</sup>

<sup>1</sup>*International Research Center “Smart materials”, Southern Federal University, 344090, 5, Zorge Str., Rostov-on-Don, Russia, <sup>2</sup>Joint Research Center “Diagnostics of structure and properties of nanomaterials”, Belgorod National Research University, 308015, 85, Pobedy Str., Belgorod, Russia*

Описана је синтеза CuO, Cu/Cu<sub>2</sub>O и Cu<sub>2</sub>O/CuO наночестица (NPs). Полазећи од дијацетатобипридинбакар(II) комплекса синтетисане су NPs применом микроталасне, солвотермалне и борхидридне методе. Због присуства бипиридинског лиганда у бакар(II) комплексу, није била неопходна додатна стабилизација овог комплекса у току синтезе. Поједиње фазе формираних NPs су идентификоване методом дифракције X-зрака. CuO NPs, димензија ≈11 nm, су добијене солвотермалном синтезом из алкалног раствора на 160 °C. Cu/Cu<sub>2</sub>O NPs, димензија ≈80 nm, су добијене помоћу микроталасне полиол методе на 185–200 °C, где овде употребљени етилен-гликол има троструку улогу, то јест као растворач, редукциони агенс и сурфактант. Cu<sub>2</sub>O/CuO NPs, димензија ≈16 nm, су синтетисане применом борхидридне методе на собној температури. Подаци за растојања између равни који су израчунати на основу одобраних површина електронских дифракција су потврдили формирање Cu, CuO и Cu<sub>2</sub>O фаза у одговарајућим узорцима. Све испитиване наночестице су стабилне и могу имати различиту примену у биомедицини.

(Примљено 11. децембра 2015, ревидирано 17. марта, прихваћено 29. марта 2016)

## REFERENCES

1. P. Lignier, R. Bellabarba, R. P. Tooze, *Chem. Soc. Rev.* **41** (2012) 1708
2. M. Yurderi, A. Bulut, I. E. Ertas, M. Zahmakiran, M. Kaya, *Appl. Catal., B* **165** (2015) 169
3. S. Mohan, Y. Singh, D. K. Verma, S. H. Hasan, *Process Saf. Environ.* **96** (2015) 156
4. M. Srivastava, J. Singh, R. K. Mishra, A. K. Ojha, *J. Alloys Compounds* **555** (2013) 123
5. S. M. Fotukian, M. N. Esfahany, *Int. Commun. Heat Mass* **37** (2010) 214
6. R. Sivaraj, P. K. S. M. Rahman, P. Rajiv, S. Narendhran, R. Venkatesh, *Spectrochim. Acta, A* **129** (2014) 178
7. A. Nowak, J. Szade, E. Talik, A. Ratuszna, M. Ostafin, J. Peszke, *Mater. Chem. Phys.* **145** (2014) 465
8. D. D. Purkayastha, N. Das, C. R. Bhattacharjee, *Mater. Lett.* **123** (2014) 206
9. M. Blosi, S. Albonetti, M. Dondi, C. Martelli, G. Baldi, *J. Nanopart. Res.* **13** (2011) 127
10. X. L. Tang, L. Ren, L.-N. Sun, W.-G. Tian, M.-H. Cao, C.-W. Hu, *Chem. Res. Chinese U.* **22** (2006) 547
11. R. Katwal, H. Kaur, G. Sharma, M. Naushad, D. Pathania, *J. Ind. Eng. Chem.* **31** (2015) 173
12. R. Sivaraj, P. K. S. M. Rahman, P. Rajiv, S. Narendhran, V. R., *Spectrochim. Acta, A* **129** (2014) 255
13. G.-J. Lee, C. K. Kim, M. K. Lee, C. K. Rhee, *Powder Technol.* **261** (2014) 143
14. A. D. Pomogailo, A. S. Rozenberg, I. E. Uflyand, *Metal Nanoparticles in Polymers*, Khimiya, Moscow, 2000, p. 672
15. Y. Wang, T. Asefa, *Langmuir* **26** (2010) 7469
16. R. Sierra-Ávila, M. Pérez-Alvarez, G. Cadenas-Pliego, V. Comparán Padilla, C. Ávila-Orta, O. P. Camacho, E. Jiménez-Regalado, E. Hernández-Hernández, R. M. Jiménez-Barrera, *J. Nanomater.* **2015** (2015), Article ID 367341
17. H. Wang, J. Xu, J.-J. Zhu, H.-Y. Chen, *J. Cryst. Growth* **244** (2002) 88
18. Y. Zhao, J.-J. Zhu, J.-M. Hong, N. Bian, H.-Y. Chen, *Eur. J. Inorg. Chem.* **2004** (2004) 4072
19. J. Xiong, Y. Wang, Q. Xue, X. Wu, *Green Chem.* **13** (2011) 900
20. O. Rubilar, M. Rai, G. Tortella, M. C. Diez, A. B. Seabra, N. Durán, *Biotechnol Lett.* **35** (2013) 1365
21. P. Ruiz, M. Muñoz, J. Macanás, D. N. Muraviev, *React. Funct. Polym.* **71** (2011) 916
22. N. Arul Dhas, C. Paul Raj, A. Gedanken, *Chem. Mater.* **10** (1998) 1446
23. H. Fan, L. Yang, W. Hua, X. Wu, Z. Wu, S. Xie, B. Zou, *Nanotechnology* **15** (2004) 37
24. W. Zhang, L. Shi, K. Tang, S. Dou, *Eur. J. Inorg. Chem.* **2010** (2010) 1103
25. S. Y. Ebrahimipour, I. Sheikhshoaie, J. Castro, W. Haase, M. Mohamadi, S. Foro, M. Sheikhshoaie, S. Esmaeili-Mahani, *Inorg. Chim. Acta* **430** (2015) 245
26. S. Medici, M. Peana, V. M. Nurchi, J. I. Lachowicz, G. Crisponi, M. A. Zoroddu, *Coordin. Chem. Rev.* **284** (2015) 329
27. B. K. Koo, *Bull. Korean Chem. Soc.* **22** (2001) 113
28. M. Abbas, B. P. Rao, S. M. Naga, M. Takahashi, *Ceram. Int.* **39** (2013) 7605
29. H. Kawasaki, Y. Kosaka, Y. Myoujin, T. Narushima, T. Yonezawa, R. Arakawa, *Chem. Commun.* **47** (2011) 7740
30. Q.-M. Liu, D.-b. Zhou, Y. Yamamoto, R. Ichino, M. Okido, *Trans. Nonferrous Met. Soc. China* **22** (2012) 117
31. G. B. Deacon, R. J. Phillips, *Coordin. Chem. Rev.* **33** (1980) 227

32. M. A. Kremennaya, M. A. Soldatov, A. P. Budnyk, T. A. Lastovina, A. V. Soldatov, *J. Struct. Chem.* (2016), accepted
33. K. Borgohain, J. B. Singh, M. V. Rama Rao, T. Shripathi, S. Mahamuni, *Phys. Rev., B* **61** (2000) 11093
34. K. Reinman, K. Syassen, *Phys. Rev., B* **39** (1989) 11113
35. G. Ren, D. Hu, E. W. Cheng, M. A. Vargas-Reus, P. Reip, R. P. Allaker, *Int. J. Antimicrob. Agents* **33** (2009) 587
36. I. Pastoriza-Santos, A. Sanchez-Iglesias, B. Rodriguez-Gonzalez, L. M. Liz-Marzan, *Small* **5** (2009) 440.